URSI GASS 2020, Rome, Italy, 29 August - 5 September 2020

Propagation Modeling inside the International Space Station for Radiofrequency Identification and Sensing of Astronauts

Nicoletta Panunzio*(1), Cecilia Occhiuzzi(1), and Gaetano Marrocco(1)
(1) University of Roma Tor Vergata, DICII, Via del Politecnico,1, 00133, Roma, Italy

Abstract

Space Agencies recognize the importance of crew health to mission success. Wireless wearable devices may provide an independent monitoring of vital signs with no human intervention. Among several options, *epidermal sensors* based on Radiofrequency Identification (RFID) are attractive for the extreme simplicity and comfort, but they offer a poor read distance. The reliability of RFID links involving epidermal antennas that are worn by astronaut is here investigated by first introducing a computational model based on Ray Tracing and then by a preliminary application to a living module of the International Space Station. Numerical results indicate that, thanks to multipath, much longer read distances than in the free space can be achieved with even the possibility to establish a communication link when reader and tags are partially in NLOS configuration.

1 Introduction

Health monitoring of astronauts is an open issue as Space Agencies already recognize the importance of crew health to mission success. At present, on-board health assessment is carried out only periodically, with questionnaires/interviews or with bulky and wired devices [1]. These systems are hence not suitable for a continuous and automatic monitoring, especially during countermeasure exercises and ordinary tasks. Moreover, they require an active involvement of crew members themselves. At the purpose to lighten the workload of astronauts and, above all, to facilitate the continuous health monitoring, there is a growing interest for autonomous wearable devices that can harvest energy from the surrounding environment and that are able to provide biophysical information without the direct intervention by the astronaut.

Ultra-High Frequency (UHF) - RFID (Radio-Frequency Identification) technology, which is widely adopted in logistics even for Space applications [2], offers nowadays even sensing capabilities without complex circuitry. In particular, UHF-RFID *epidermal sensors* [3] are used to monitor physical parameters, such as temperature, blood pressure, oxygen level, electrophysiology, and more recently they are also able to detect biomarkers in sweat [4, 5, 6].

A challenge for the continuous monitoring is the limited read range of state-of-the-art battery-less epidermal RFID sensors (70 cm - 1.5 m, at most, in open field) [7]. Accordingly, the reliability of this platform in a Space environment needs to be demonstrated yet. As a Space capsule, like the International Space Station (ISS), is a highly scattering environment, the usual free-space link does not apply, and a more accurate propagation model must be identified. In particular, a typical space module scenario consists of a tunnel-like large structure, enclosed by a metallic reflective fuselage, populated by a variable number of floating people. This leads to waveguide effects, signal distortion, and multipath, making this a complex propagation environment, too much computationally intensive for conventional Full Wave (FW) tools based on FDTD, FEM or MOM methods. On the contrary, an asymptotic approach based on Ray Tracing (RT) may provide a reasonable balance between accuracy and computational time when multipath propagation in complex indoor environments is involved. In comparison with indoor radiowave propagation, the Astronaut problem includes the additional challenge of a backscattering antenna placed onto the human skin and, hence, it deserves an ad hoc approach.

The purpose of this paper is to identify the most suitable modeling strategy to account for both the scattering of the metallic environment and the presence of the human body on which the RFID tag is placed. For this purpose, three computational methods, having different complexity and accuracy, are compared by application to a benchmark scenario. The most effective model is then applied inside the ISS for a preliminary analysis of the RFID link, considering epidermal tags put in different positions over three phantoms, in turn distributed in different locations inside an ISS module.

2 Statement of the problem

The benchmark configuration (Fig. 1) comprises an homogeneous human phantom with relative permittivity $\varepsilon = 43$ and electric conductivity $\sigma = 0.9\ S/m$ [7], modeled as an elliptical cylinder ($1.65\ m$ height, 25 and 40 cm diameters). For simplicity, the epidermal RFID tag is a copper dipole (length $= 15\ cm$ [7], maximum radiation gain in the broadside $G_{tag,max} = -12\ dBi$). The tag is placed over the phantom at an height of $82.5\ cm$. To account for multipath effects, a $2 \times 2\ m$ PEC plate is placed behind the phantom, at a distance of $1\ m$. Finally, the reader is emulated by a linear polarized patch antenna, perfectly matched (maximum radiation gain in the broadside $G_{R,max} = 6.7\ dBi$, power transfer coefficient $\tau_R = 1$), placed at a distance of $2\ m$ from the body. The mutual orientation of the two antennas is such that their polarizations are parallel (polarization loss factor $\eta_P = 1$).

In a preliminary test (Benchmark A), only the presence of the body without the plate is considered. The phantom (with the on-body tag) is gradually rotated around its axis ($\alpha = \{0°, 20°\ 30°, 45°, 90°\}$) to investigate the effect of misalignment between tag and reader's antenna.
In a second simulation campaign (Benchmark B), also the reflecting plate is considered, with orientations that produce both LOS (Line of Sight) and NLOS (Non Line of Sight) links.
The performance indicator is the power that the reader delivers to the tag and is hence collected by the tag's IC ($P_{R\to T}$) for various mutual orientations between body, reader and plate. This is the key parameter to estimate the establishment of a reliable RFID link as the epidermal tag is activated when $P_{R\to T} > P_{o,chip}$, being $P_{o,chip}$ the microchip power sensitivity.

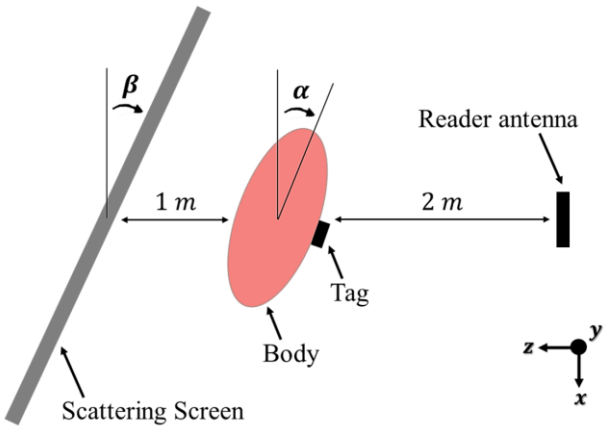

Figure 1. Benchmark for the RFID link evaluation, involving skin-mounted antennas and scattering objects nearby.

Three computational models are here considered: a Full Wave (FW) method, to be referred as reference model, the Friis scheme, and a Ray Tracer (RT).

2.1 Full Wave modeling by FDTD and Two-Port Network Model

The Two-Port Network Model is based on the idea that the system consisting of the reader and on-body tag can be reviewed as a two-port network, where the reader's generator is connected to the input port, while the tag's IC, is connected to the output port. This model provides an easy way to determine the power collected by the IC as:

$$P_{R\to T} = G_T\, P_{av,G}\,, \qquad (1)$$

where $P_{av,G}$ is the input available power at the reader's port, and G_T is the system's transducer power gain, defined as in [8]. The impedance matrix $[Z]$, that is required to calculate G_T, is numerically computed by a FW simulation of the whole system including reader's antenna, tag and phantom, and the reflector screen (when present).

This approach accounts for all the electromagnetic interactions, but is computationally hard when size increases.

2.2 Friis Link

According to the free-space assumption (Friis link), instead, the amount of power collected by the RFID tag's IC, when it is illuminated by a reader antenna, is estimated as:

$$P_{R\to T} = P_{av,G}\, G_{tag} G_R \left(\frac{\lambda}{4\pi d}\right)^2 \tau_{tag}\, \tau_R\, \eta_P\,, \qquad (2)$$

where d is the reader-tag distance, $\{G_{tag}, \tau_{tag}\}$ are the tag's gain and radiation power transmission coefficient, and $\{G_R, \tau_R\}$ represent the corresponding parameters of the reader's antenna. These quantities need to be derived from two separate FW simulations, one involving the only reader's antenna in the free space, and the other involving the phantom+tag system, still in free space. Accordingly, the Friis model ignores the mutual interactions between the elements of the scenario and, in particular, it is unable to account for the scattering effect of the body and of the reflecting screen.

2.3 Ray Tracing modeling

The Ray Tracing approach involves only the far field of the reader's antenna (offline evaluated once and for all by any FW method). The human body is still modeled as a uniform cylinder as above, but it is accounted only for the reflected rays, so that penetration and absorption of the electromagnetic field are not considered. The interaction with the epidermal tag, not included in the model, is instead accounted for by means of the following procedure, aiming at deriving the power delivered to the IC.
From the RT simulation, the Poynting vector $\underline{S}(\underline{r_{IC}}) = \frac{1}{2}\,\underline{E}(\underline{r_{IC}}) \times \underline{H}^*(\underline{r_{IC}})$ is evaluated in the position $(\underline{r_{IC}})$ of the body where the tag's IC is supposed to be placed. Then, the power received by the chip is simply estimated as:

$$P_{R\to T} = |S|\, A_{tag}\, \tau_{tag}\, \eta_P\,, \qquad (3)$$

where η_P is the polarization loss factor (PLF), depending on the relative orientation of transmitter and tag's polarization, while $A_{tag} = \lambda^2 G_{tag}/4\pi$ is the effective area of the tag, that again needs to be derived from a FW simulation in which only the phantom+tag system is modeled.
Unlike the Friis-based estimation, here the scattering from both the body and the environment is taken into account. Several tag positions over the body, as well as rotations of the body itself, can be derived from a same RT simulation.

3 Benchmark Results

All the simulations mentioned above are performed with DESSAUT - MICROWAVE STUDIO 2019, by using the FDTD solver (as FW method) and the Asymptotic solver (as RT method).

3.1 Benchmark A (without the plate)

Apart from the $\alpha = 0°$ case, the tag's gain to insert in the formulas is estimated as a mean value inside the $-3dB$ beamwidth ($\overline{G}_{tag,-3dB} = -13.2\ dBi$).
Table I shows a good agreement between the FW and RT outcomes for all the considered orientations. In the absence of a scattering wall, Friis model returns an overestimation with respect to the FW model, as reader/body interaction is neglected.

3.2 Benchmark B (including the plate)

In NLOS case, the tag's gain to insert in the Friis Formula is collected along the line joining the reader's antenna and the tag ($G_{tag,NLOS} = -32.8\ dBi$). For the RT simulations, instead, tag's gain is averaged within both the $-3dB$ beamwidth (*case a*: $\overline{G}_{tag,-3dB} = -13.2\ dBi$) and the $-6dB$ beamwidth (*case b*: $\overline{G}_{tag,-6dB} = -14.1\ dBi$).
Table II demonstrates that the RT model still provides coherent results with respect to the FW, even in NLOS case with a maximum error of 3 dB in case of $\overline{G}_{tag,-6dB}$. The Friis Formula, instead, is inapplicable in the presence of the screen, as expected.

Table I. Power on chip estimation comparison: $\boldsymbol{P_{R\to T}}$ [$\boldsymbol{dBm}$]. No PEC plate.

	Friis Formula	Two-Port Network Model (FWM)	Ray Tracing
$\boldsymbol{\alpha = 0°}$	-20.0	-21.6	-21.0
$\boldsymbol{\alpha = 20°}$	-20.9	-23.1	-24.7
$\boldsymbol{\alpha = 30°}$	-20.9	-22.6	-24.7
$\boldsymbol{\alpha = 45°}$	-21.0	-22.8	-23.6
$\boldsymbol{\alpha = 90°}$	-21.4	-27.1	-26.0

Table II. Power on chip estimation comparison: $\boldsymbol{P_{R\to T}}$ [$\boldsymbol{dBm}$]. With PEC plate.

	Friis Formula	Two-Port Network Model (FWM)	Ray Tracing
LOS $\boldsymbol{\alpha = 0°}$ $\boldsymbol{\beta = 0°}$	-20.0	-20.0	-20.3
NLOS $\boldsymbol{\alpha = 270°}$ $\boldsymbol{\beta = 25°}$	-41.5	-30.7	-26.2 (a) -27.1 (b)

The RT model can be hence considered as a valuable tool to predict the RFID link, also when on-body tags are involved, with a moderate computational burden (*78 s* against *1345 s* of the FW method[1]).

4 Application to ISS: *Harmony* Module

The RT model is here applied inside a semi-closed environment resembling the *Node 2* (*Harmony*) module (Fig. 2a) of the International Space Station. The simplified model consists of a PEC fuselage shell, with an overall length of about 7.9 m and a width of about 2.6 m [9]. The reader's antenna is now a circular polarized patch antenna ($G_{R,max} = 7.0\ dBi$, $\overline{G}_{R,-3dB} = 5.7\ dBi$, $\tau_R = 1$) placed at the closed (left) end of the module (Fig. 2b).

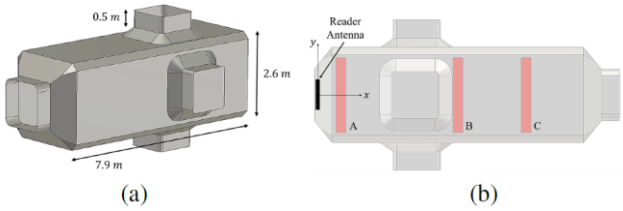

Figure 2. (a) Simplified model of ISS *Harmony* module. (b) Detail of the position of the reader's antenna and of the phantom. Reader's antenna not in scale.

The reference epidermal tag is now a $3 \times 3\ cm$ thin-wire open loop (realized gain $G_{tag}\tau_{tag} = -15\ dBi$, chip sensitivity $P_{o,chip} = -16.6\ dBm$), derived from [10] and suitable for temperature monitoring. This tag is assumed to be placed at different positions over the body (from 1 to 12 in Fig. 3), thus producing both LOS and NLOS links. Three body phantoms are located as in Fig. 3 at increasing distances from the reader $d \cong \{0.7\ m, 4\ m, 6\ m\}$.

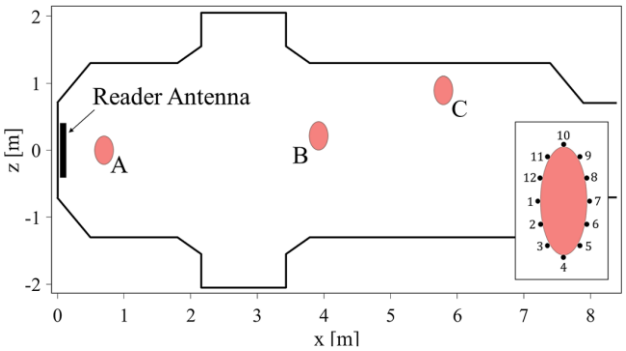

Figure 3. Horizontal cross-section of the *Harmony* module with indication of three cylindrical body model's positions. Reader's antenna not in scale. Inset: N.12 positions of the tag over the bodies.

Fig. 4a shows the estimated distribution map of the Poynting vector inside the module in the absence of people, assuming the reader is emitting 4 $W\ EIRP$, according to FCC

[1] Computer technical specifications: Microsoft Windows 10 Home, 64-bit; Intel(R) Core(TM) i7-8700K CPU @ 3.70GHz, 3701 MHz, 6 Core(s), 12 Logical Processor(s); 32 GB RAM; NVIDIA GeForce GTX 1070.

regulations (§15.247). Fringes are visible as the effect of multipath, with a cut-off around 2.5 m from the reader's antenna.

The power delivered to the tag's IC for all the considered configurations and positions is finally resumed in Fig. 4b. In the position A, closest to the reader ($d = 0.7\ m$), the power is nearly always higher than the IC sensitivity, and hence the RFID link is reliable against the position of the tag and against the mutual orientation of the body (as it may happen during the astronaut hovering). In the intermediate position B, the RFID link can be still activated, mostly when reader and tag are in LOS condition. And, it is worth noticing that, thanks to multipath, this reader-body distance ($d = 4\ m$) is 4-5 times longer than the maximum reading range of epidermal tags in free space. Finally, in the most remote position C ($d = 6\ m$), the power collected by the chip is not enough for activation even in LOS cases.

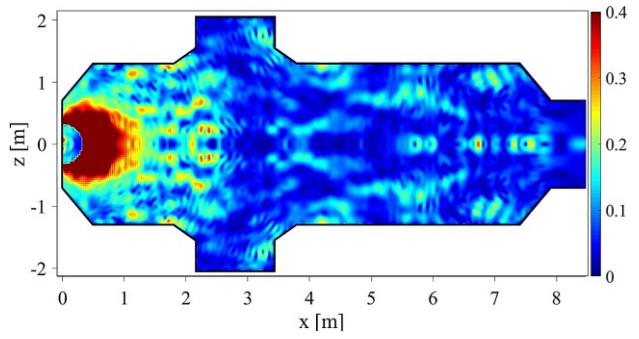

(a)

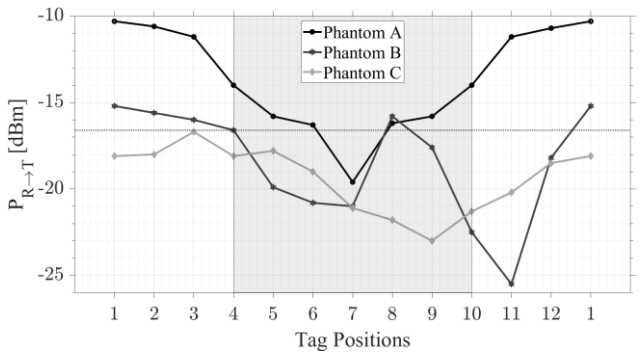

(b)

Figure 4. (a) Distribution of the Poyinting vector's magnitude [W/m^2] over an horizontal cross-section of the ISS module, corresponding to a radiated power of 4 $W\ EIRP$. (b) Estimated Power on chip for the three phantoms and for increasing angle of placements of the tags as in Fig. 3. The gray area highlights the NLOS cases. The dotted horizontal line indicates the power activation threshold ($P_{o,chip} = -16.6\ dBm$).

5 Conclusions

A numerical procedure, based on the Ray Tracing, has been proposed for the estimation of the reliability of an RFID link involving epidermal antennas worn by astronauts. A preliminary analysis inside a module of the International Space Station demonstrated that, thanks to the multipath, a reliable continuous reading, practically independent from the orientation of the astronaut, looks feasible when he is up to about 1 m far from the reader, as when he is crossing a gate between two modules. For longer distances, sporadic reading could be however achieved also up to the middle of the module. A more uniform link, hence, requires the installation of multiple reader's antennas, as it will be shown at the Symposium together with a statistic analysis.

References

[1] NASA. https://www.nasa.gov/sites/default/files/atoms/files/np-2017-04-014-jsc_iss_utilization_brochure_2017_human_physiology_adaptation.pdf.

[2] E. C. Jones, C. Richards, K. Herstein, R. Franca, E. L. Yagoda, and R. Vasquez, *RFID in Space: Exploring the Feasibility and Performance of Gen 2 Tags as a Means of Tracking Equipment, Supplies, and Consumable Products in Cargo Transport Bags onboard a Space Vehicle or Habitat.* October 2008.

[3] G. Marrocco, "RFID antennas for the UHF remote monitoring of human subjects," *Antennas and Propagation, IEEE Transactions on*, vol. 55, pp. 1862 – 1870, July 2007.

[4] S. Amendola, G. Bovesecchi, A. Palombi, P. Coppa, and G. Marrocco, "Design, Calibration and Experimentation of an Epidermal RFID Sensor for Remote Temperature Monitoring," *IEEE Sensors Journal*, vol. 16, pp. 1–1, October 2016.

[5] C. Miozzi, S. Nappi, S. Amendola, C. Occhiuzzi, and G. Marrocco, "A General-Purpose Configurable RFID Epidermal Board with a Two-Way Discrete Impedance Tuning," *IEEE Antennas and Wireless Propagation Letters*, vol. PP, pp. 1–1, February 2019.

[6] S. Nappi, V. Mazzaracchio, L. Fiore, F. Arduini, and G. Marrocco, "Flexible pH Sensor for Wireless Monitoring of the Human Skin from the Medium Distances," pp. 1–3, July 2019.

[7] S. Amendola and G. Marrocco, "Optimal Performance of Epidermal Antennas for UHF Radio Frequency Identification and Sensing," *IEEE Transactions on Antennas and Propagation*, vol. PP, pp. 1–1, December 2016.

[8] S. J. Orfanidis, *Electromagnetic Waves and Antennas.* August 2016.

[9] NASA, *Reference Guide to the International Space Station.* September 2015.

[10] F. Amato, C. Miozzi, S. Nappi, and G. Marrocco, "Self-Tuning UHF Epidermal Antennas," *IEEE Inter-national Conference on RFID Technology and Applications (RFID-TA)*, 2019.